Available online at www.sciencedirect.com
ScienceDirect
Trans. Nonferrous Met. Soc. China 31(2021) 317−330
Transactions of Nonferrous Metals Society of China
www.tnmsc.cn

Improved wettability and mechanical properties of metal coated carbon fiber-reinforced aluminum matrix composites by squeeze melt infiltration technique

Jian-jun SHA[1,2], Zhao-zhao LÜ[1,2], Ru-yi SHA[1,2], Yu-fei ZU[1,2], Ji-xiang DAI[1,2], Yu-qiang XIAN[3], Wei ZHANG[3], Ding CUI[3], Cong-lin YAN[3]

1. State Key Laboratory of Structural Analyses for Industrial Equipment, Dalian University of Technology, Dalian 116024, China;
2. Key Laboratory of Advanced Technology for Aerospace Vehicles, Liaoning Province, Dalian University of Technology, Dalian 116024, China;
3. Institute of Applied Electronics, China Academy of Engineering Physics, Mianyang 621900, China

Received 29 March 2020; accepted 11 November 2020

Abstract: In order to improve the wettability and bonding performance of the interface between carbon fiber and aluminum matrix, nickel- and copper-coated carbon fiber-reinforced aluminum matrix composites were fabricated by the squeeze melt infiltration technique. The interface wettability, microstructure and mechanical properties of the composites were compared and investigated. Compared with the uncoated fiber-reinforced aluminum matrix composite, the microstructure analysis indicated that the coatings significantly improved the wettability and effectively inhibited the interface reaction between carbon fiber and aluminum matrix during the process. Under the same processing condition, aluminum melt was easy to infiltrate into the copper-coated fiber bundles. Furthermore, the inhibited interface reaction was more conducive to maintain the original strength of fiber and improve the fiber−matrix interface bonding performance. The mechanical properties were evaluated by uniaxial tensile test. The yield strength, ultimate tensile strength and elastic modulus of the copper-coated carbon fiber-reinforced aluminum matrix composite were about 124 MPa, 140 MPa and 82 GPa, respectively. In the case of nickel-coated carbon fiber-reinforced aluminum matrix composite, the yield strength, ultimate tensile strength and elastic modulus were about 60 MPa, 70 MPa and 79 GPa, respectively. The excellent mechanical properties for copper-coated fiber-reinforced composites are attributed to better compactness of the matrix and better fiber−matrix interface bonding, which favor the load transfer ability from aluminam matrix to carbon fiber under the loading state, giving full play to the bearing role of carbon fiber.
Key words: carbon fiber; metal matrix composite; C_f/Al composite; coating; wettability; mechanical properties

1 Introduction

It is well known that carbon fiber (C_f) has been one of the most ideal reinforcements for different kinds of composites because of its excellent mechanical and chemical stabilities [1,2]. Aluminum-based alloys are important engineering materials for the lightmass structures. However, there are some limitations for aluminum-based alloys subjected to some specific applications such as aerospace and military vehicles. In order to further improve the comprehensive properties of aluminum-based alloys, incorporating carbon fiber into the aluminum and forming the carbon fiber-reinforced aluminum-based matrix composites are a preferring choice [3,4]. It is expected that composites combining the excellent mechanical properties of carbon fiber with the

Corresponding author: Jian-jun SHA; Tel: +86-411-84709004; E-mail: jjsha@dlut.edu.cn
DOI: 10.1016/S1003-6326(21)65498-5
1003-6326/© 2021 The Nonferrous Metals Society of China. Published by Elsevier Ltd & Science Press

excellent ductility of aluminum alloys would have a high priority for using in the advanced lightmass structures.

Therefore, recently carbon fiber-reinforced aluminum matrix composites have been considered as the advanced lightmass structural materials for aerospace and other civil industries due to their high specific strength/modulus, high anti-vibration resistance, low coefficient of thermal expansion and good thermal conductivity [5]. However, one of the major issues is the poor wettability between carbon fiber and aluminum matrix during the fabrication of composites [6]. The poor wettability leads to the difficulty for the infiltration of aluminum melt into the intra-bundle area of carbon fiber. Although increasing the process temperature can improve the wettability between carbon fiber and aluminum matrix to some extent, the unavoidable interface reaction between carbon fiber and aluminum matrix may happen and form the aluminum carbide (Al_4C_3) phase which is naturally brittle. The brittle Al_4C_3 phase and the strongly bonded fiber−matrix interface resulted from interface reaction may affect the mechanical properties of composites [7,8]. In order to alleviate the interface reaction and improve the wettability between carbon fiber and aluminum matrix, the surface modification of carbon fiber can be an effective method. Particularly, to fabricate an appropriate coating on the carbon fiber has been demonstrated to be an effective approach for improving the wettability and inhibiting the interface reaction [9−13].

A great effort has been made to develop the coating technology on carbon fiber. Generally, carbon fiber with metallic or ceramic coating is often used to reinforce the aluminum matrix composites. In Refs. [9−11], nickel (Ni) and copper (Cu) coatings were deposited on the surface of carbon fiber by chemical plating technique, and the coated fiber was used as the reinforcement for the fabrication of aluminum matrix composites. The results indicated that the coatings could effectively improve the wetting behavior between the carbon fiber and aluminum melt. And also, the carbon fiber coated with ceramics such as the alumina and silicon carbide was used to fabricate the aluminum matrix composite [12,13]. The results were really encouraging and the formation of Al_4C_3 at the interface between the aluminum matrix and carbon fiber was refrained by the ceramic coatings. However, taking the engineering application into consideration, the realistic problems are the high cost and complex process to fabricate the ceramic coating on the surface of carbon fiber on a large scale. On the other hand, the ceramic coatings might have a negative effect on the deformation ability of aluminum matrix composites due to their brittle nature. Thus, metallic coatings would be more suitable for the fabrication of carbon fiber-reinforced aluminum matrix composites because of their high flexibility and good compatibility with aluminum matrix. Considering the cost efficiency, the electroplating process is a simple and inexpensive technology and presents a weak impact on the environment compared with the chemical plating and other technologies [14].

During the last decade, some fabrication techniques such as powder metallurgy, gas pressure infiltration and squeeze casting were developed as the main processing routes to prepare composites [15−17]. Each processing route presented some merits in fabrication of the composite. As for the reinforcement, the large aspect ratio is promising due to its versatile strengthening and toughening mechanisms, such as fiber pull-out, interface debonding, crack deflection and fiber bridging.

Therefore, in the current work, the un-coated, Ni- and Cu-coated continuous carbon fibers were used to fabricate composites by the squeeze melt infiltration technique under vacuum condition. The use of continuous carbon fiber can consume more work than that of short ones when they are pulled out from the matrix, which would increase the strength/toughness of the composites. The effects of Ni and Cu coating on wettability, microstructure and mechanical properties of composites were investigated. The scanning electron microscopy (SEM) was used to characterize the microstructure and morphology of the coatings and composites. The X-ray diffractometer (XRD) with energy dispersive spectrometer (EDS) was utilized to characterize the phase constitutions and elements, respectively. The mechanical properties were measured by uniaxial tension test.

2 Experimental

2.1 Materials

A commercially available PAN-based carbon

fiber (C_f: T-300, supplied by Toray Company, Japan) was used as the reinforcement. Commercial aluminum sheets (purity higher than 99%, supplied by Southwest Aluminum Company, China) were used as the matrix. Acidic nickel and copper electroplating solutions were used as the Ni and Cu sources to deposit the Ni and Cu coatings on the carbon fiber, respectively. The chemical reagents and the compositions of electroplating solutions for the deposition of Ni and Cu coatings are presented in Table 1.

The reason for the selection of partial chemical reagents can refer to Ref. [14]. In order to separate the fiber from the bundle and improve the surface conductivity of carbon fiber in electroplating solutions, the desizing was performed by treating the fiber in acetone solution and heating at 673 K for 30 min in a muffle furnace under ambient atmosphere.

2.2 Deposition of Ni and Cu coatings on carbon fiber

The carbon fiber is inclined to agglomerate together in a bundle, which may lead to inhomogeneous deposition of coating on carbon fiber [18]. To improve the coating efficiency and the quality, a double-anode electroplating system assisted with ultra-sonic oscillator was applied to depositing the Ni and Cu coatings on carbon fiber. In both cases, with the assistance of ultra-sonic vibration, the fiber bundles became loose, which would be helpful not only for the homogeneous deposition of coating, but also for the later infiltration of Al melt into fiber bundles. In previous researches [19−21], the effects of electroplating parameters on the deposition quality of each coating were systematically investigated. In this work, the coating was fabricated using the optimized deposition condition based on the previous results.

Figure 1 shows the schematic diagram of experimental setup used for the electroplating of Ni and Cu coatings on carbon fiber, where carbon fiber tows acted as the cathode and were placed in the middle of two Ni or Cu anodes in an electroplating bath. During the electroplating, the steady electrical current was supplied to the Ni or Cu anodes and the C_f cathode. Both coating depositions were conducted at room temperature with controlled electroplating parameters (for Ni coating: pH=4, time 8 min, current density 0.6 A/dm^2; for Cu coating: pH=1, time 8 min, current density 0.8 A/dm^2).

2.3 Fabrication of composites

The composites were fabricated by the squeeze melt infiltration technique under vacuum condition. By this technique, the molten aluminum can not only infiltrate into the C_f bundle well by applied pressure, but also avoid the oxidation of the aluminum and carbon fiber.

Figure 2(a) shows the schematic illustration for the squeeze melt infiltration technique and the direction of the applied load. The aluminum was slightly treated with the low concentration acidic solutions to remove the oxide layer formed on the surface of aluminum. The oxide layer usually impedes the flowing of aluminum melt. The treated aluminum was put on the carbon fiber with Ni and Cu coatings and confined in a graphite die. The fiber's volume fraction was about 8% in this work. Finally, the graphite die was moved into the furnace chamber and heated at 943 K for 20 min under vacuum condition. During heating, a load

Table 1 Chemical reagents and compositions of electroplating solutions for deposition of Ni and Cu coatings

Solution	Reagent	Molecular formula	Concentration/(g·L^{-1})
Ni coating	Nickel sulfate	$NiSO_4·6H_2O$	123
	Boracic acid	H_3BO_3	30
	Nickel chloride	$NiCl_2·6H_2O$	32
	Sodium dodecyl sulfate	$CH_3(CH_2)_{11}OSO_3Na$	0.12
Cu coating	Copper sulfate pentahydrate	$CuSO_4·5H_2O$	80
	Sulfuric acid	H_2SO_4	68
	Copper chloride	$CuCl_2$	0.24
	Sodium 3,3′-dithiodipropane sulfonate	$C_6H_{12}O_6S_4Na_2$	0.025
	OP emulsifier	OP-10	0.4

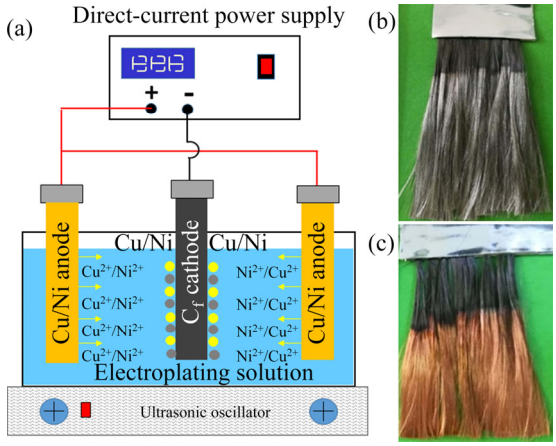

Fig. 1 Schematic diagram of experiment setup for deposition of Ni and Cu coatings on carbon fiber (a), carbon fiber with Ni coating (b) and carbon fiber with Cu coating (c)

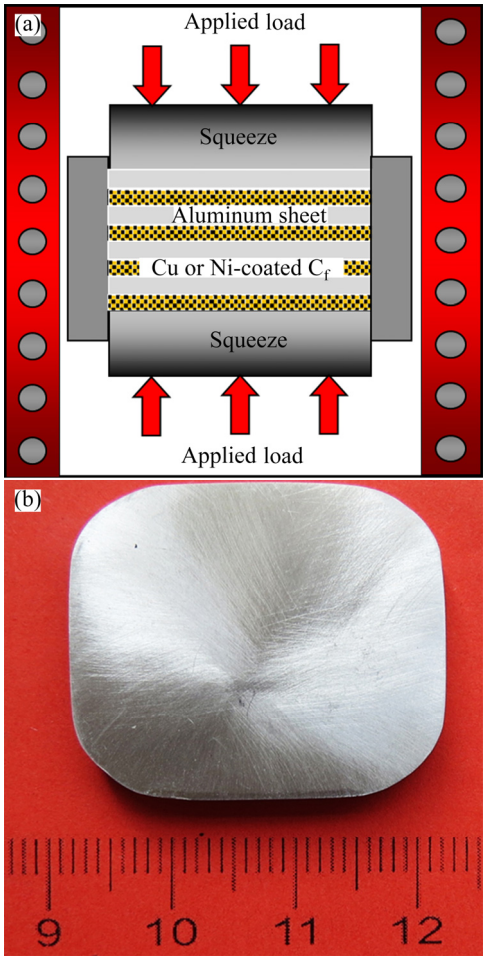

Fig. 2 Schematic illustration of squeeze melt infiltration technique (a) and macro-image of C_f–Cu/Al composite polished roughly (b)

of 15 MPa was applied to the aluminum and carbon fiber. The load was maintained until the furnace cooling to room temperature. Hereafter, for identifying different composites, the un-coated, Cu-coated and Ni-coated carbon fiber-reinforced aluminum composites were referred as the C_f/Al, C_f–Cu/Al and C_f–Ni/Al composites, respectively. Figure 2(b) shows the macro-image of the fabricated C_f–Cu/Al composite, which was taken out from the graphite die and polished roughly.

2.4 Characterization

The phase constitutions of composites were characterized by means of the X-ray diffractometer. The bulk density of composites was measured by Archimedes method. The relative density was determined by dividing the measured density by the theoretical density. The influence of Ni and Cu coatings on the wettability between carbon fiber and aluminum matrix was analyzed by the SEM equipped with EDS. The tensile properties of the composites were evaluated by a universal mechanical testing machine (Model: WDW−100) with a constant strain rate of 10^{-3} s^{-1} at room temperature following the standard ASTM D3552—12. The composites were machined into a dog-bone shape specimen. For each composite, the mean value was obtained from 3 tests. The fracture surfaces were observed by SEM to characterize the fracture features.

3 Results and discussion

3.1 Ni and Cu coatings on carbon fiber

The as-received carbon fiber generally presents a smooth surface because of the presence of the sizing on the surface of carbon fiber as shown in Fig. 3(a). The sizing is a kind of organic material with low electronic conductivity, which will act as the barrier for the electron transmission. Particularly, in the electroplating solution, the sizing will decrease the electrical conductivity of carbon fiber and has a negative effect on the deposition efficiency and the quality of coatings. Thus, it is quite necessary to remove the surface sizing. Figure 3(b) shows the surface morphology of carbon fiber after desizing. The surfaces of carbon fiber presented a textured structure with clear grooves. It is also found from SEM observation that the diameters of carbon fiber before and after desizing have no visible change. Using carbon fiber with and without the sizing, a comparative investigation on the coating deposition was carried

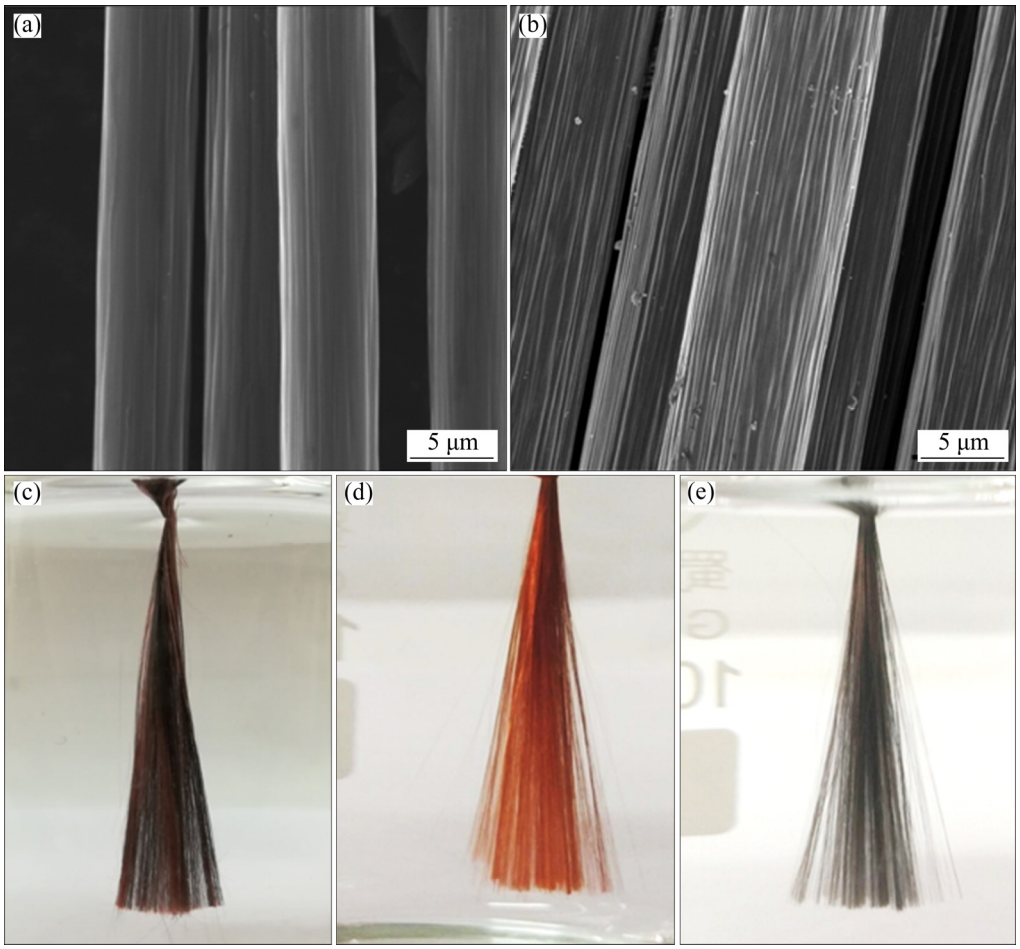

Fig. 3 SEM images of carbon fiber before (a) and after (b) desizing, macro-images of Cu coatings deposited on carbon fiber with (c) and without (d) sizing, and Ni coating deposited on carbon fiber without sizing (e)

out. Figure 3(c) shows a macro-image of Cu-coated fiber bundle with sizing. The surface of the fiber tow is not so bright and the quality of Cu coating seems poor. The low brightness is attributed to the non-homogeneous deposition of Cu coating. This is due to the fact that the existence of sizing has a high electrical resistance and the Cu coating is difficult to deposit on the surface of fibers. In contrast, for the desized carbon fibers, after deposition of the coatings, they present uniform and shining surfaces with different colors as shown in Figs. 3(d) and (e).

Figure 4 shows the morphologies of different coatings on carbon fiber observed by SEM. From the surface morphologies of Ni- and Cu-coated carbon fiber as shown in Figs. 4(a) and (b), it can be seen that Ni and Cu were homogeneously electroplated on the surfaces of carbon fiber. Along the length direction of the fiber, the surface image presented a flat and straight profile, which indicated that a continuous and uniform coating was formed on the carbon fiber. Only a small difference was that the surface of Ni-coated fiber was somewhat rougher than that of Cu-coated fiber. Moreover, from the cross-sections of fibers with Ni and Cu coatings as shown in Figs. 4(c) and (d), respectively, it can be seen that the coating and fiber formed a core−shell structure. The thickness of Ni and Cu coatings was about 1.3 μm and the coatings were firmly adhered on the surface of carbon fiber. From these observations, again it was confirmed that the smooth and continuous metallic coating with a uniform thickness was deposited on carbon fiber by the present process. The main reason for the formation of high quality coating could be attributed to the fiber's desizing and ultrasonic vibration dispersion, which can make the carbon fiber completely contact with the electroplating solution. On the other hand, the electroplating additives also play an important role in the quality of coatings. The addition of $NiCl_2·6H_2O$ and $CuCl_2$

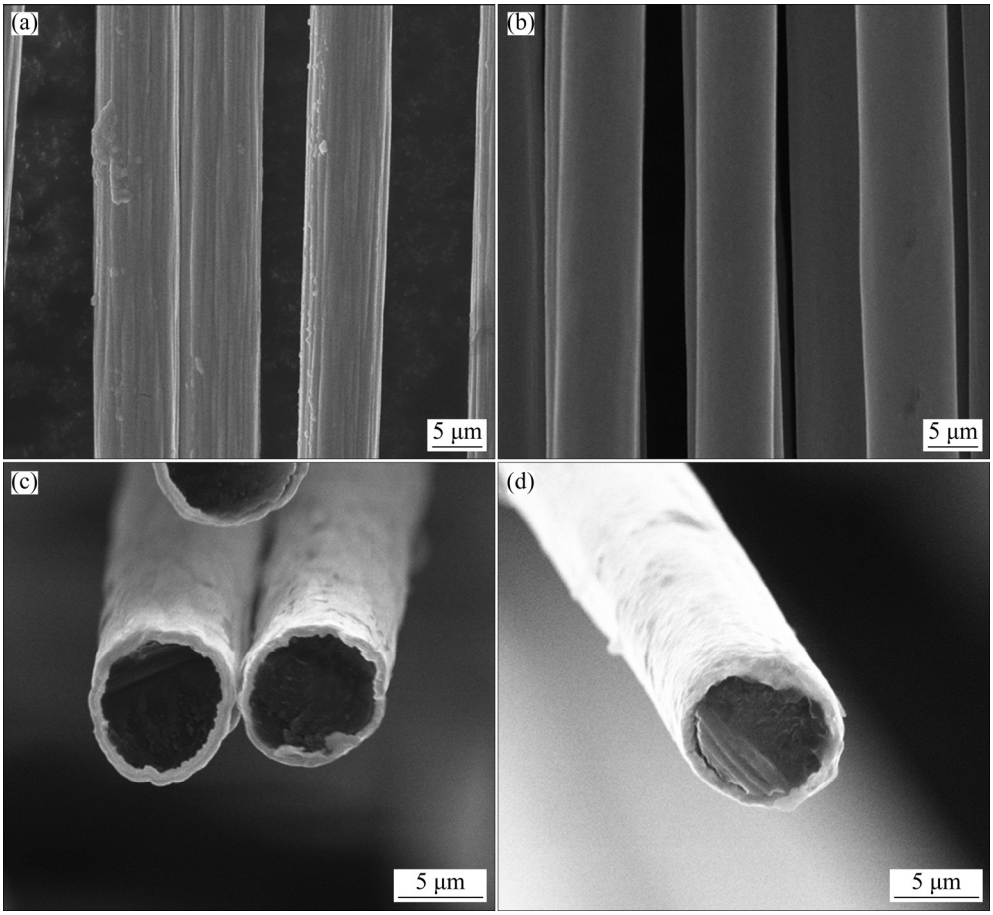

Fig. 4 SEM images of Ni- and Cu-coated carbon fiber: (a) Surface of Ni-coated carbon fiber; (b) Surface of Cu-coated carbon fiber; (c) Cross-section of Ni-coated carbon fiber; (d) Cross-section of Cu-coated carbon fiber

in electroplating solutions can keep the activation of Ni and Cu anodes during the electroplating process. Particularly, the Cl^- generated from the additives ($NiCl_2·6H_2O$ and $CuCl_2$) can inhibit the production of O_2 which can oxidize Ni^{2+}/Cu^{2+} and form the insoluble Ni_2O_3/CuO_2 in the electroplating solutions [14]. The solid Ni_2O_3/CuO_2 particles can deposit on both Ni/Cu anodes and carbon fiber cathode. If Ni_2O_3/CuO_2 particles deposit on the Ni/Cu anodes, they will prevent the Ni/Cu anodes from dissolving and the electroplating process will be compelled to stop. If $Ni{-}Ni_2O_3$ or $Cu{-}CuO_2$ co-deposits on the carbon fiber, it will increase the internal stress of coatings and decrease the brightness, resulting in a rough coating surface. $CH_3(CH_2)_{11}OSO_3Na$ and OP-10 can reduce the surface tension stress between electrode and electroplating solution. Furthermore, during the electroplating process, H^+ is reduced and the amount of H_2 bubbles formed on the carbon fiber cathode becomes small. H_2 bubble acting as a barrier can stop the deposition of Ni and Cu on carbon fiber. $CH_3(CH_2)_{11}OSO_3Na$ and OP-10 can adsorb on carbon fiber and decrease the surface energy between carbon fiber and solution, making the H_2 bubbles hardly adsorbed on carbon fiber [22,23]. Additionally, $C_6H_{12}O_6S_4Na_2$ acting as a brightener, can be also adsorbed on the surface of carbon fiber cathode. The $C_6H_{12}O_6S_4Na_2$ enlarges the electrochemical polarization of carbon fiber, which could refine the grain size of Cu coating.

3.2 Microstructure and phase constitution

In order to know the influence of Ni and Cu coatings on the wettability of interface between carbon fiber and Al, the microstructures of composites were observed. Figure 5 shows the SEM micrographs of composites. In case of the C_f/Al composite as shown in Fig. 5(a), a dense Al matrix was observed, but a great number of pores appeared in the area of fiber bundles. The wettability is quite dependent on the contact angle of Al melt and carbon fiber. Due to the poor wettability between Al melt and carbon fiber, a

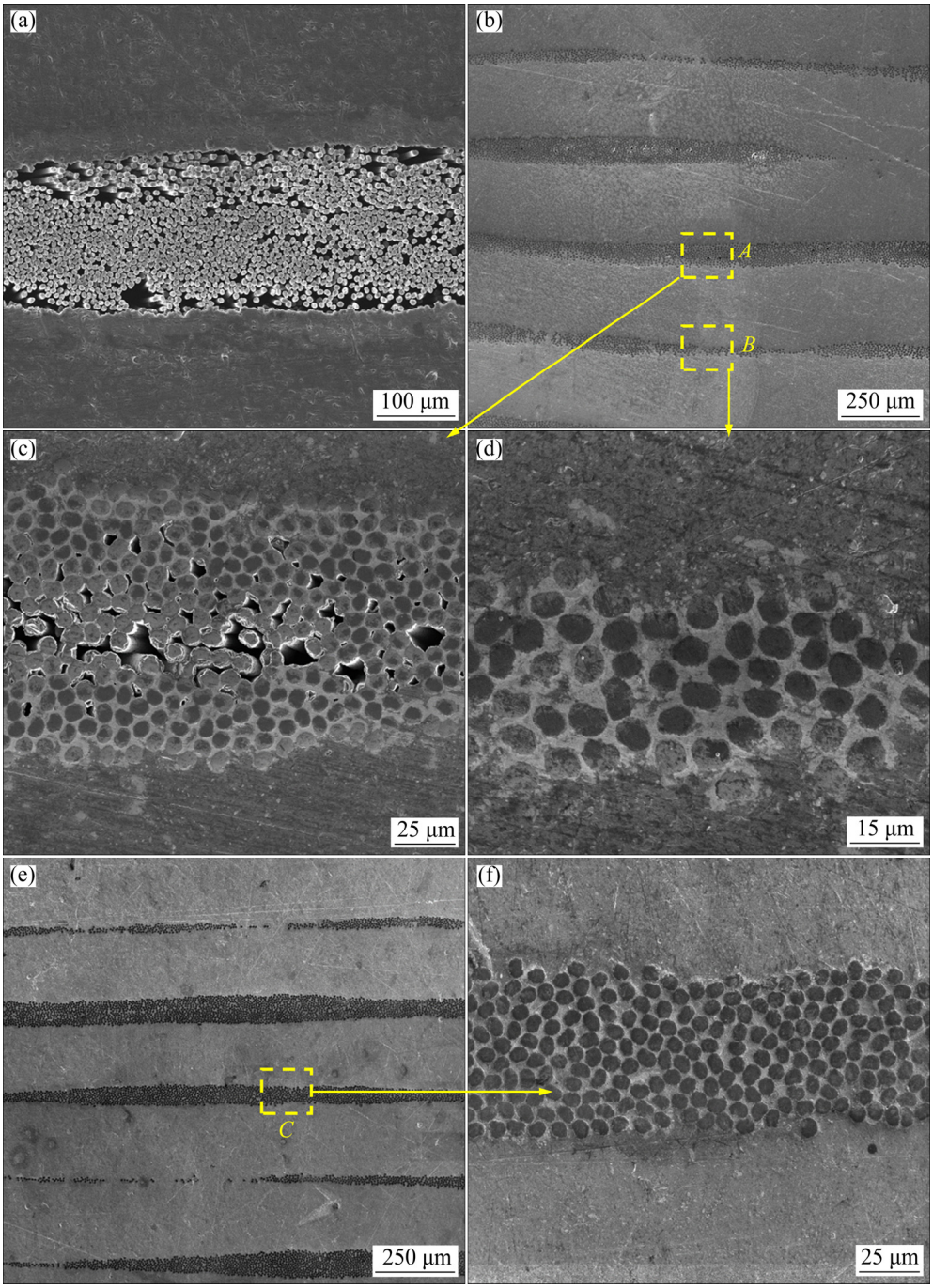

Fig. 5 SEM micrographs of composites: (a) C_f/Al composite; (b) C_f–Ni/Al composite; (c) Magnified image of selected area *A* in (b); (d) Magnified image of selected area *B* in (b); (e) C_f–Cu/Al composite; (f) Magnified image of selected area *C* in (e)

large contact angle would be formed at the interface. Based on the theoretic investigation, when the contact angle is greater than the threshold contact angle of spontaneous infiltration, the melt is not easy to infiltrate into the fibrous preform [24]. With the support of this knowledge, the contact angle of carbon fiber and Al should be larger than the threshold value, resulting in the generation of anti-spreading force. Such force expels the Al melt from the intra-bundle area, leading to a poor infiltration behavior as shown in Fig. 5(a). As for the C_f–Ni/Al composites (Fig. 5(b)), the infiltration behavior is affected by the local volume fraction of carbon fiber. For the area with high fiber volume fraction, although some micro-pores are found in the central area of intra-fiber bundle, most of fiber bundles are embedded in aluminum matrix as shown in the selected area *A* (Fig. 5(c)). The

existence of the micropores might be caused by the high melting point of Ni. On the other hand, the micropores could act as the structural defects and affect the mechanical properties of composites. For the area with small fiber volume fraction, the fiber intra-bundle areas are well infiltrated with the Al as shown in the selected area *B* (Fig. 5(d)). For the C_f–Cu/Al composite shown in Fig. 5(e), both inter-bundle area and intra-bundle area are very dense (Fig. 5(f)). The carbon fiber incorporates very well with the Al matrix, and no apparent pores and defects are found in intra-bundle areas shown in Fig. 5(e).

Based on the microstructure observations, it could be easily found that both Ni and Cu coatings significantly improved the wettability between carbon fiber and Al matrix. This was because the wetting took place under chemical non-equilibrium condition. The chemical non-equilibrium developed because both the solid and liquid phases were unsaturated with respect to each other, and the formation of the compounds occurred at the interface [25,26]. In the present work, during the fabrication, the Ni and Cu coatings dissolved into the Al melt and formed the liquid solutions. Simultaneously, the fiber's surface exposed to the melt directly improved the wettability [27,28].

Although both Ni and Cu coatings could improve the infiltration behavior of Al melt, Cu coating is better than Ni. Probably, the following mechanism would be responsible for this phenomenon. According to the Al−Ni phase diagram, Ni became saturated in the Al melt when the Ni concentration reached about 8 wt.% at 943 K [29]. Upon saturation, the intermetallic phase would be precipitated, which may prevent further infiltration of Al melt into fiber bundles. For the Cu dissolving into the Al melt, the saturation concentration was as high as 62 wt.% at 943 K. Therefore, the Al melt could completely infiltrate into the fiber bundles.

Figure 6 shows the XRD patterns for different specimens. For carbon fiber, only a broaden peak at 2θ of 26.5° was observed. The broadening of carbon peak was attributed to the low graphitization of carbon fiber. The T300 carbon fiber usually has a disordered graphite structure because of low processing temperature (1573−1773 K) resulting in low graphitization degree [30]. For pure Al, only one phase appeared. For the C_f–Ni/Al and C_f–Cu/Al composites, besides the diffraction peaks of Ni and Al phases, the diffraction peaks for the intermetallic compounds Al_3Ni and Al_2Cu were also clearly observed, respectively. The peak for brittle Al_4C_3 phase was not detected, which was viewed as the harmful phase and often appeared in the C_f/Al composites. In the current work, the formation of Al_4C_3 was suppressed. The suppression of Al_4C_3 could be associated with the Ni and Cu coatings on carbon fiber. When the Al melt is formed, the dissolution and diffusion of Ni and Cu from coatings can form the liquid solutions and intermetallic compounds with Al melt, which act as the isolation barrier against the dissolution of carbon atoms and the reaction between carbon fiber and Al melt [9,31]. Therefore, the Ni and Cu coatings not only improved the wettability between carbon fiber and Al matrix, but also suppressed the formation of harmful phase Al_4C_3.

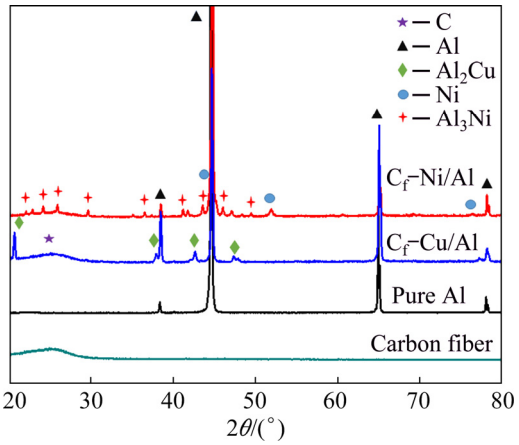

Fig. 6 XDR patterns of different specimens

To further know the influence of coatings on the wettability and microstructure, the EDS mapping was performed on the cross-section of composites. Figure 7 shows EDS mapping of the cross-sections of C_f–Ni/Al and C_f–Cu/Al composites. For C_f–Ni/Al composite, the Ni-rich phase around the carbon fiber was clearly observed as shown in Figs. 7(a) and (c), and it was proved to be Al_3Ni phase by XRD in Fig. 6. From Fig. 7(b), it was evidenced that the molten Al infiltrated into the intra-bundle area of fibers and contacted with the Ni under pressure. Simultaneously, the Ni dissolved into Al melt and formed the Al_3Ni. When the Ni reached the saturation state, the Al_3Ni precipitated at the interface between carbon fiber and Al. The precipitated Al_3Ni around carbon fiber might slow

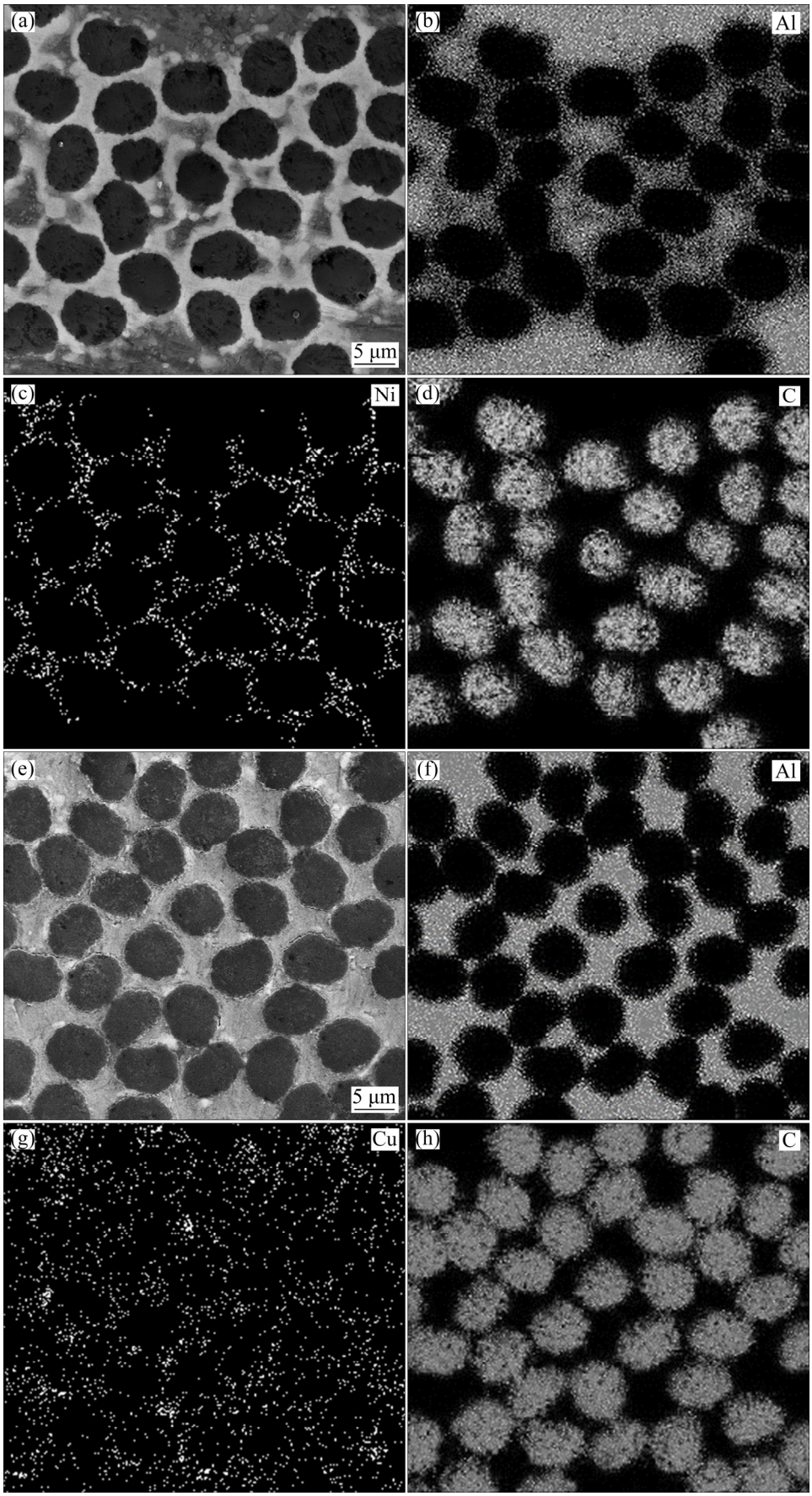

Fig. 7 EDS mappings of cross-sections of composites: (a−d) C_f–Ni/Al composite; (e−h) C_f–Cu/Al composite

down the infiltration of melt into the intra-bundle area, resulting in the formation of micro-pores. However, in the case of C_f–Cu/Al composite as shown in Figs. 7(e–h), the Al melt completely infiltrated into the intra-bundle area of fiber, which was evidenced by the high intensity of Al in Fig. 7(f). It is unlike Ni coating that almost all Cu coatings diffused into Al matrix as shown in Fig. 7(g), and some light spots near the interface of fiber and matrix in Fig. 7(g) convinced the formation of intermetallic compound Al_2Cu observed in Fig. 6. It seems that the diffusion modes for Ni and Cu are different in the Al matrix, which would lead to different influences on wettability and properties of composites. According to the classical Arrhenius equation, the diffusion coefficient of Ni and Cu in the Al can be written as

$$D = D_0 \exp\left(-\frac{Q}{RT}\right)$$

where D_0 is the frequency factor (m^2/s), Q is the activation energy (J/mol), R is the molar gas constant (8.314 J/(mol·K)), and T is the thermodynamic temperature (K). The diffusion coefficient of Cu coating in Al is 2.45×10^{-13} m^2/s at 943 K [32], and that of Ni coating in Al is 6.58×10^{-16} m^2/s at 943 K [33]. Therefore, compared with Ni coating, Cu coating is easier to diffuse into Al at the processing temperature. This is consistent with the observed phenomenon.

3.3 Mechanical properties and fracture characteristics

Using the stress–strain curves, the tensile properties were calculated and listed in Table 2. The yield strength, ultimate tensile strength and elastic modulus of the C_f–Ni/Al composite are about 60 MPa, 70 MPa and 79 GPa, respectively. The yield strength, ultimate tensile strength and elastic modulus of the C_f–Cu/Al composite are about 124 MPa, 140 MPa and 82 GPa, respectively. The ultimate tensile strength and yield strength of C_f–Cu/Al composite are almost twice as those of C_f–Ni/Al composite. The mechanical properties of both composites are much higher than those of pure Al. As we know, Cu is a cheaper metal compared to Ni. Thus, the current result can lay a foundation for further development of Al-based matrix composites. Due to a good bonding at the interface between the carbon fiber and the Al matrix, the elongations of the C_f–Cu/Al composite and the C_f–Ni/Al composite reach 8.1% and 19.8%, respectively.

Figure 8 shows the SEM micrographs of fracture surfaces for C_f–Ni/Al and C_f–Cu/Al composites. Some micro-cracks could be found in the C_f–Ni/Al composite as shown in Figs. 8(a) and (b). The cracks were mainly located in the intra-bundle area. It seemed that the propagation of cracks was along the fiber bundle. The formation and propagation of micro-cracks could be related to the stress state and the existence of micro-pores formed during the fabrication process. In Fig. 5, it was found that the micro-pores appeared in the inner area of fiber bundles. Such micro-pores as the structural defects easily led to the pull-out of carbon fiber, and they were prone to cause the stress concentration during the tensile test. On the other hand, because of the formation of Al_3Ni around carbon fiber, it enhanced the interfacial strength and made the C_f–Ni/Al composite relatively brittle [34,35]. These were the main reasons why the C_f–Ni/Al composite exhibited a lower tensile strength compared to the C_f–Cu/Al composite. In the case of C_f–Cu/Al composite as shown in Figs. 8(c) and (d), because the Cu coating promoted the wettability between the carbon fiber and Al better than Ni coating, the Al melt was well infiltrated into the fiber bundle areas and made a modest interface bonding. Compared with the C_f–Ni/Al composite, the number and size of micro-cracks in C_f–Cu/Al composite were much less, and the fracture surfaces of C_f–Cu/Al composite were rather rough. Furthermore, the crack density and crack width were also smaller than those of C_f–Ni/Al composite.

Figure 9 shows SEM micrographs of the

Table 2 Mechanical properties of different materials

Material	Density/ ($g\cdot cm^{-3}$)	Relative density/%	Ultimate tensile strength/MPa	Elastic modulus/GPa	Yield strength/ MPa	Elongation/ %
Pure Al	2.70	100	54.5±5.1	69.6±3.7	42.2±2.9	29.7
C_f–Ni/Al	2.60	99.0	70.4±4.6	78.5±1.0	59.5±2.3	19.8
C_f–Cu/Al	2.62	99.8	140.3±8.7	81.5±2.2	123.5±1.5	8.1

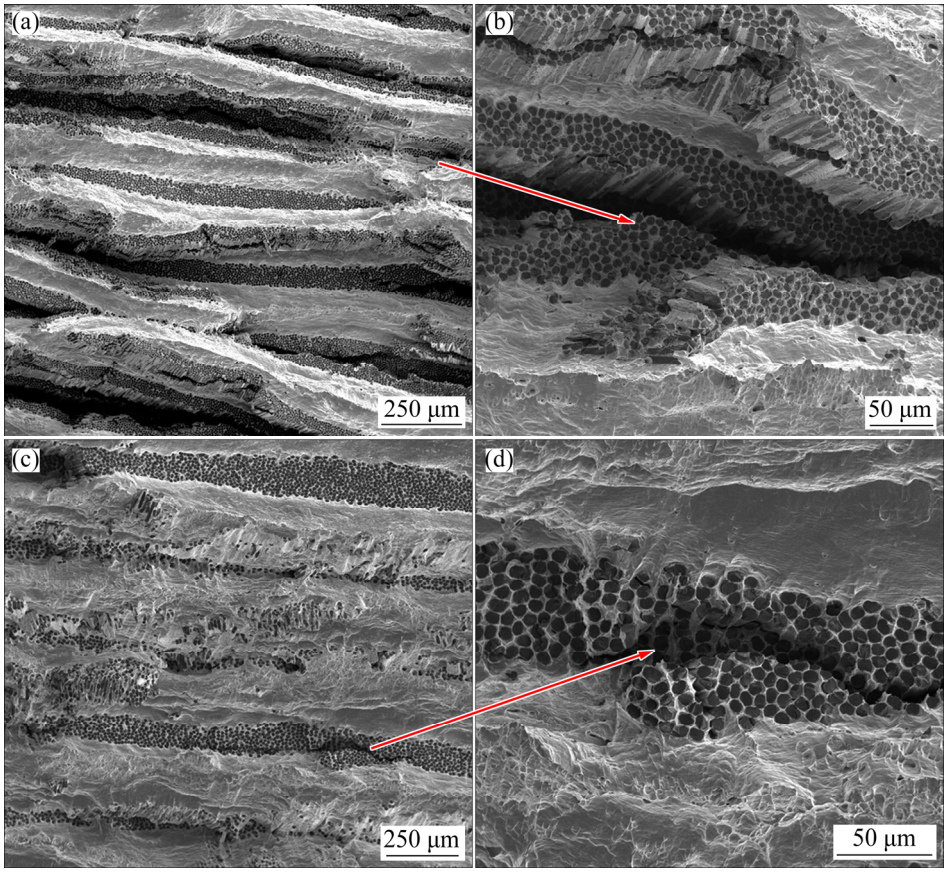

Fig. 8 SEM micrographs of fracture surfaces of composites: (a, b) C_f–Ni/Al composite; (c, d) C_f–Cu/Al composite

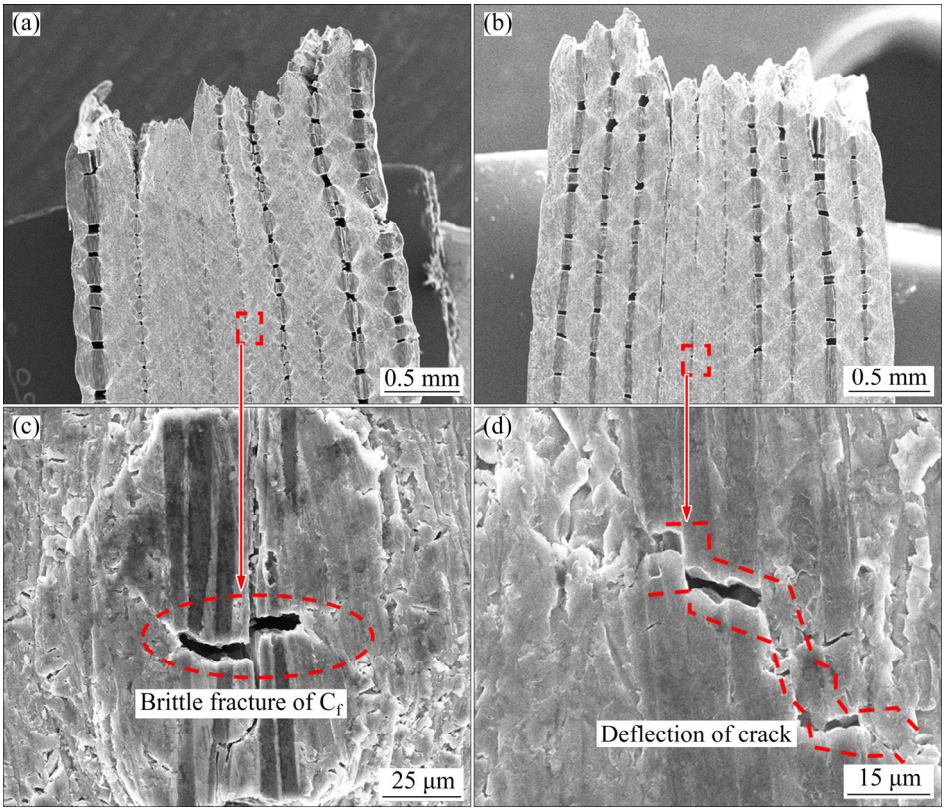

Fig. 9 SEM micrographs of lateral surfaces of composites after tensile tests: (a, c) C_f–Ni/Al composites; (b, d) C_f–Cu/Al composites

lateral surfaces of specimens after tensile tests. It could be found that the profiles of fracture surfaces in both composites presented zigzag shape, as shown in Figs. 9(a) and (b). The formation of the zigzag profiles could be attributed to different deformation ability between carbon fiber and Al matrix. It is well known that the failure strain of carbon fiber is much smaller than that of aluminum. This is consistent with the observed phenomenon that the intra-bundle area shows lower elongation than that of the inter-bundle area. Furthermore, if we carefully observe the lateral surfaces of the fractured specimens, it can be seen that the intra-bundle areas are broken into many small segments with a length about 0.16 mm (Fig. 9(a)). In contrast, for the C_f–Cu/Al composite, the length of segments formed by the fracture of intra-bundle areas is about 0.25 mm (Fig. 9(b)). This is because the failure strain of carbon fiber is much smaller than that of the aluminum matrix. Therefore, the continuous release of the fracture energy during the tension would lead to the formation of fiber bundle fragments, which confirmed that carbon fiber played a very important role in the mechanical properties of the composites. During the tension, the load was effectively transferred from the Al matrix to carbon fiber. Due to large difference in deformation ability between carbon fiber and Al matrix, at the tension state, the load was mainly borne by the carbon fiber. With continuous increase of tensile strain, the rupture of carbon fiber would be possible. Subsequently, the fiber−matrix interface debonding, sliding and even the fiber's pull-out led to the fragment formation. The length of fragment should be related to the interface bonding state and the fiber−matrix bonding strength. On the other hand, the plastic deformation of the matrix may absorb part of the fracture energy and hinder the propagation of cracks. And also, the plastic deformation can weaken the stress concentration, thus resulting in the stress redistribution until carbon fiber failed [7].

4 Conclusions

(1) The microstructure analysis of composites revealed that both Ni and Cu coatings can not only improve the wettability between carbon fiber and Al matrix, but can also act as the isolation barrier at interface, which suppress the formation of brittle phase Al_4C_3 from the interface reaction. The Cu coating presents better wettability and interface bonding than Ni coating in the current processing condition.

(2) The improved wettability and interface bonding between carbon fiber and Al matrix in the C_f–Cu/Al composite could be attributed to the high diffusion coefficient of Cu in Al. Better wettability and interface bonding favor the load transfer ability from matrix to fiber under the loading state.

(3) The yield strength, ultimate tensile strength and elastic modulus of the C_f–Cu/Al composite are about 124 MPa, 140 MPa and 82 GPa, respectively. The yield strength and ultimate tensile strength the C_f–Cu/Al composite are almost twice as those of C_f–Ni/Al composite. Furthermore, the C_f–Ni/Al composite exhibits better elongation than C_f–Cu/Al composite.

Acknowledgments

The authors are grateful for the financial supports from Joint Fund of the National Natural Science Foundation of China and the China Academy of Engineering Physics (U1630129).

References

[1] CHAND S J. Review carbon fibers for composites [J]. Journal of Materials Science, 2000, 35: 1303−1313.

[2] SHIRVANIMOGHADDAM K, HAMIM S U, AKBARI M K, FAKHRHOSEINI S M. Carbon fiber reinforced metal matrix composites: Fabrication processes and properties [J]. Composites: Part A, 2017, 92: 70−96.

[3] BAUML P, SYCHEV J, BUDAI I, SZABO J T, KAPTAY G. Fabrication of carbon fiber reinforced aluminum matrix composites via a titanium-ion containing flux [J]. Composites: Part A, 2013, 44: 47−50.

[4] JUHASZ K L, BAUML P，KAPTAY G. Fabrication of carbon fibre reinforced aluminum matrix composite by potassium iodide (KI)−potassium hexafluoro-titanate (K_2TiF_6) flux [J]. Materialwissenschaft und Werkstofftechnik, 2012, 43: 310−314.

[5] RAWAL S P. Metal-matrix composites for space applications [J]. JOM, 2001, 53: 14−17.

[6] MATSUNAGA T, MATSUDA K, HATAYAMA T, SHINOZAKI K, YOSHIDA M. Fabrication of continuous carbon fiber-reinforced aluminum–magnesium alloy composite wires using ultrasonic infiltration method [J]. Composites: Part A, 2007, 38: 1902−1911.

[7] ZHANG Yun-he, WU Gao-hui. Interface and thermal expansion of carbon fiber reinforced aluminum matrix composites [J]. Transactions of Nonferrous Metals Society of China, 2010, 20: 2148−2151.

[8] DENG Chun-feng, ZHANG Xue-xi, WANG De-zun.

Chemical stability of carbon nanotubes in the 2024 Al matrix [J]. Materials Letters, 2007, 61: 904−907.

[9] HAJJARI E, DIVANDARI M, MIRHABIBI A R. The effect of applied pressure on fracture surface and tensile properties of nickel coated continuous carbon fiber reinforced aluminum composites fabricated by squeeze casting [J]. Materials and Design, 2010, 31: 2381−2386.

[10] YANG Qiu-rong, LIU Jin-xu, LI Shu-kui, WANG Fu-chi, WU Teng-teng. Fabrication and mechanical properties of Cu-coated woven carbon fibers reinforced aluminum alloy composite [J]. Materials and Design, 2014, 57: 442−448.

[11] DAOUD A. Microstructure and tensile properties of 2014 Al alloy reinforced with continuous carbon fibers manufactured by gas pressure infiltration [J]. Materials Science and Engineering A, 2005, 391: 114−120.

[12] TANG Yi-ping, DENG Yi-da, ZHANG Kai, LIU Liu, WU Ya-ting, HU Wen-bin. Improvement of interface between Al and short carbon fibers by α-Al_2O_3 coatings deposited by sol–gel technology [J]. Ceramics International, 2008, 34: 1787−1790.

[13] LEE C W, KIM L H, LEE W, KO S H, JIANG J M, LEE T W, LIM S H, PARK J P, KIM J D. Formation and analysis of SiC coating layer on carbon short fiber [J]. Surface and Interface Analysis, 2010, 42: 1231−1234.

[14] HUA Zhong-sheng, LIU Yi-han, YAO Guang-chun, WANG Lei, MA Jia, LIANG Li-si. Preparation and characterization of nickel-coated carbon fibers by electroplating [J]. Journal of Materials Engineering and Performance, 2012, 21: 324−330.

[15] SILVAIN J F, VEILLERE A, LU Y F. Copper−carbon and aluminum−carbon composites fabricated by powder metallurgy processes [J]. Journal of Physics: Conference Series, 2014, 525: 012015.

[16] YANG J Y, CHUNG D D L. Casting particulate and fibrous metal-matrix composites by vacuum infiltration of a liquid metal under an inert gas pressure [J]. Journal of Materials Science, 1989, 24: 3605−3612.

[17] ZHANG Xue-xi, YANG Li, DENG Chun-feng, WANG De-zun. Multi-wall carbon nanotubes reinforced aluminum composites synthesized by hot press sintering and squeeze casting [J]. Transactions of Nonferrous Metals Society of China, 2006, 16: 1465−1469.

[18] LU Guang-hong, LI Xiao-tian, JIANG Han-cheng. Electrical and shielding properties of ABS resin filled with nickel-coated carbon fibers [J]. Composites Science and Technology, 1996, 56: 193−200.

[19] LV Zhao-zhao, SHA Jian-jun, ZU Yu-fei, LIN Guan-zhang DAI Ji-xiang. Influences of electroplating parameters on deposition of Ni coatings on carbon fibers by electroplating technique assisted with ultrasonic vibration [J]. The Chinese Journal of Nonferrous Metals, 2020, 30: 571−579. (in Chinese)

[20] LV Zhao-zhao, SHA Jian-jun, LIN Guan-zhang, ZHANG Zhao-fu, ZU Yu-fei. Deposition of Cu on carbon fibers and influence mechanisms [J]. Rare Metal Materials and Engineering, 2019, 48: 4010−4015. (in Chinese)

[21] LV Zhao-zhao, ZU Yu-fei, SHA Jian-jun, XIAN Yu-qiang, ZHANG Wei. Fabrication and mechanical properties of carbon fiber-reinforced aluminum matrix composites with Cu interphase [J]. Acta Metallurgica Sinica, 2019, 55: 317−324. (in Chinese)

[22] TAN M, HARD J N. Additive behavior during copper electrodeposition in solutions containing Cl^-, PEG, and SPS [J]. Journal of the Electrochemical Society, 2003, 150: C420−C425.

[23] TAO Zhi-hua, HE Wei, WANG Shou-xu, HE Xue-mei, JIAO Cheng, XIAO Ding-jun. Synergistic effect of different additives on microvia filling in an acidic copper plating solution [J]. Journal of the Electrochemical Society, 2016, 163: 379−384.

[24] KAPTAY G. The threshold pressure of infiltration into fibrous preforms normal to the fibers' axes [J]. Composites Science and Technology, 2008, 68: 228−237.

[25] IP S W, SRIDHAR R, TOGURI J M, STEPHENSON T F, WARNER A E M. Wettability of nickel coated graphite by aluminum [J]. Materials Science and Engineering A, 1998, 244(1): 31−38.

[26] OH S I, LIM J Y, KIM Y C, YOON J, KIM G H, LEE J, SUNG Y M, HAN J H. Fabrication of carbon nanofiber reinforced aluminum alloy nanocomposites by a liquid process [J]. Journal of Alloys and Compounds 2012, 542: 111−117.

[27] RAJAN T P D, PILLAL R M, PAL B C, Review reinforcement coatings and interfaces in aluminium metal matrix composites [J]. Journal of Materials Science, 1998, 33: 3491−3503.

[28] TANAKA Y, KAJIHARA M, WATANABE Y. Growth behavior of compound layers during reactive diffusion between solid Cu and liquid Al [J]. Materials Science and Engineering A, 2007, 445: 355−363.

[29] ZHANG Z X, JIANG H, RUSSELL A M, SKROTZKI W, MULLER E, SCHNEIDER R, GERTHSEN D, CAO G H. Microstructural evolution and phase transformation in the liquid−solid Al/Ni diffusion couple [J]. Philosophical Magazine, 2019, 99: 1−18.

[30] SHA Jian-jun, DAI Ji-xiang, WEI Zhi-qiang, HAUSHERR J M, KRENKEL W. Influence of thermal treatment on thermo-mechanical stability and surface composition of carbon fiber [J]. Applied Surface Science, 2013, 274: 89−94.

[31] SILVAIN J F, PROULT A, LAHAYE M, DOUIN J. Microstructure and chemical analysis of C/Cu/Al interfacial zones [J]. Composites: Part A, 2003, 34: 1143−1149.

[32] ZHANG Lian-meng, HUANG Xue-hui, SONG Xiao-lan. Fundamentals of materials science [M]. 2nd ed. Wuhan: Wuhan University of Technology Press, 2008. (in Chinese)

[33] HIRANO K I, AGARWALA R P, COHEN M. Diffusion of iron, nickel and cobalt in aluminum [J]. Acta Metallurgica, 1962, 10: 857−863.

[34] SUZUKI T, UMEHARA H, HAYASHI R, WATANABE S. Mechanical properties and metallography of aluminum matrix composites reinforced by the Cu- or Ni-plating carbon multifllament [J]. Journal of Materials Research, 1993, 8: 2492−2498.

[35] URENA A, RAMS J, ESCALERA M D, SANCHEZ M. Characterization of interfacial mechanical properties in carbon fiber/aluminium matrix composites by the nanoindentation technique [J]. Composites Science and Technology, 2005, 65: 2025−2038.

挤压熔体浸渗法制备金属涂覆碳纤维增强铝基复合材料的润湿性和力学性能改善

沙建军[1,2]，吕钊钊[1,2]，沙如意[1,2]，祖宇飞[1,2]，
代吉祥[1,2]，鲜玉强[3]，张 伟[3]，崔 鼎[3]，严从林[3]

1. 大连理工大学 工业装备结构分析国家重点实验室，大连 116024；
2. 大连理工大学 辽宁省空天飞行器前沿技术重点实验室，大连 116024；
3. 中国工程物理研究院 应用电子学研究所，绵阳 621900

摘 要：为了改善碳纤维与铝基体之间界面的润湿性和结合性能，采用挤压熔体浸渗法制备镍和铜涂覆碳纤维增强铝基复合材料，对两种不同涂层碳纤维增强铝基复合材料的界面润湿性、显微组织和力学性能进行比较和研究。显微组织结构分析表明，与无涂层碳纤维增强铝基复合材料相比，在相同的浸渗工艺条件下，在碳纤维表面涂覆两种金属均可以显著改善碳纤维与铝基体间的润湿性，铝熔体容易进入纤维束内部；两种金属界面层涂覆在铝熔体浸渗期间均可有效抑制碳纤维与铝基体间的界面化学反应，从而更有利于保持碳纤维的原始强度和改善纤维−基体界面结合性能。单轴拉伸力学性能研究结果表明，铜涂覆碳纤维增强铝基复合材料的屈服强度、极限抗拉强度和弹性模量分别约为 124 MPa、140 MPa 和 82 GPa；镍涂覆碳纤维增强铝基复合材料的屈服强度、极限抗拉强度和弹性模量分别约为 60 MPa、70 MPa 和 79 GPa。铜涂覆碳纤维增强铝基复合材料比镍涂覆碳纤维增强铝基复合材料具有更优性能。这是由于铜具有较低的熔点，在挤压熔渗过程中易形成致密的基体和良好的纤维−基体结合界面，从而使加载过程中的载荷容易从铝基体传输到碳纤维，充分发挥碳纤维的承载作用。

关键词：碳纤维；金属基复合材料；C_f/Al 复合材料；涂层；润湿性；力学性能

(Edited by Wei-ping CHEN)